

Generalized Constitutive Relations for Metamaterials Based on the Quasi-Static Lorentz Theory

Akira Ishimaru, *Life Fellow, IEEE*, Seung-Woo Lee, Yasuo Kuga, *Senior Member, IEEE*, and Vikram Jandhyala, *Member, IEEE*

Abstract—This paper presents a method of calculating the elements of the generalized matrix representation of the macroscopic constitutive relations for a three-dimensional (3-D) array of nonmagnetic inclusions with arbitrary shape. The derivation is based on the quasi-static Lorentz theory and the inclusions are represented by electric and magnetic dipole moments. The 6×6 constitutive relation matrix is expressed in terms of the interaction matrix and the polarizability matrix, which can be numerically calculated using the sum and the difference of opposing plane wave excitations. Numerical examples are given for split ring resonators and a chiral medium consisting of an array of helices to illustrate the usefulness of the formula and to verify the consistency constraint and reciprocity relations for a bianisotropic medium.

Index Terms—Anisotropic media, chirality, composite materials, metamaterials, microwave materials, periodic structures, permeability, permittivity.

I. INTRODUCTION

IN recent years, there has been an increasing interest in the development of new materials with characteristics which may not be found in nature. Examples are metamaterials [1], [2], left-handed media [3]–[7], composite media [8], [9], and chiral media [10]–[16]. They have a broad range of applications including artificial dielectrics, lens, absorbers, antenna structures, optical and microwave components, frequency selective surfaces, and composite materials. In addition, left-handed material has a negative refractive index, its permeability and permittivity are both negative, and was conjectured to be capable of producing a perfect lens [4], although its limitations have been pointed out [7], [17].

In these applications, it is important to describe the material characteristics in terms of the physical properties of the inclusions. This paper presents a generalized matrix representation of the macroscopic constitutive relations for a three-dimensional (3-D) periodic array of nonmagnetic inclusions based on the quasi-static Lorentz theory. The macroscopic constitutive relations are given by

$$\begin{bmatrix} \bar{D} \\ \bar{B} \end{bmatrix} = \begin{bmatrix} \bar{\epsilon} & \bar{\xi} \\ \bar{\zeta} & \bar{\mu} \end{bmatrix} \begin{bmatrix} \bar{E} \\ \bar{H} \end{bmatrix} \quad (1)$$

where $\bar{\epsilon}$, $\bar{\xi}$, $\bar{\zeta}$, and $\bar{\mu}$ are 3×3 matrices. Equation (1) is applicable to linear medium, and is often called the E - H (or Tel-

legen) representation. It is convenient as the Maxwell equations appear symmetric and boundary conditions are generally given in terms of \bar{E} and \bar{H} [18], [19]. Note, however, that physically \bar{E} and \bar{B} are the fundamental fields and \bar{D} and \bar{H} are the derived fields related to \bar{E} and \bar{B} through constitutive relations [19]. Therefore, in the E - B (or Boys-Post) representation, we have

$$\begin{bmatrix} \bar{D} \\ \bar{H} \end{bmatrix} = \begin{bmatrix} \bar{\epsilon}_p & \bar{\alpha}_p \\ \bar{\beta}_p & \bar{\mu}_p^{-1} \end{bmatrix} \begin{bmatrix} \bar{E} \\ \bar{B} \end{bmatrix}. \quad (2)$$

Equations (1) and (2) are equivalent for linear medium and related through the following:

$$\begin{aligned} \bar{\epsilon} &= \bar{\epsilon}_p - \bar{\alpha}_p \bar{\mu}_p^{-1} \bar{\beta}_p, & \bar{\mu} &= \bar{\mu}_p \\ \bar{\xi} &= \bar{\alpha}_p \bar{\mu}_p, & \bar{\zeta} &= -\bar{\beta}_p \bar{\mu}_p. \end{aligned} \quad (3)$$

The medium with the constitutive relation (1) is called the “bianisotropic medium” [11], [20], [21]. If $\bar{\epsilon}$, $\bar{\xi}$, $\bar{\zeta}$, and $\bar{\mu}$ are scalars, this is called the “bi-isotropic” or “chiral” medium.

It has been shown [18], [22] that for the constitutive relations of the bianisotropic medium to be compatible with Maxwell’s equations, the following consistency constraint holds:

$$\text{Trace}([\bar{\xi}][\bar{\mu}]^{-1} + [\bar{\mu}]^{-1}[\bar{\zeta}]) = 0 \quad (4)$$

in the E - H formulation.

It has also been shown [19] that the constitutive relations for the bianisotropic nongyrotropic medium satisfy the following reciprocity relations.

$$\begin{aligned} [\bar{\epsilon}]^t &= [\bar{\epsilon}], & [\bar{\mu}]^t &= [\bar{\mu}] \\ [\bar{\xi}]^t &= -[\bar{\zeta}] \end{aligned} \quad (5)$$

where t denotes transpose.

These relations (4) and (5) are useful to verify the accuracy of the calculations as explained in Section VIII.

There are two important questions. First is how to obtain these parameters $\bar{\epsilon}$, $\bar{\xi}$, $\bar{\zeta}$, and $\bar{\mu}$ for a given material. The second is how to describe the wave characteristics in such a medium.

In this paper, we address the first question. We derive the explicit expressions of these matrix parameters for a given configuration of the inclusions in a host material. The inclusions are arranged in a 3-D array and consist of nonmagnetic materials with complex dielectric constants. The derivation is based on the quasi-static Lorentz theory and, therefore, applicable to inclusions whose sizes and spacings are small compared with

Manuscript received July 19, 2002; revised November 20, 2002. This work was supported by the National Science Foundation (ECS-9908849).

The authors are with the Department of Electrical Engineering, University of Washington, Seattle, WA 98195 USA (e-mail: ishmaru@ee.washington.edu).

Digital Object Identifier 10.1109/TAP.2003.817565

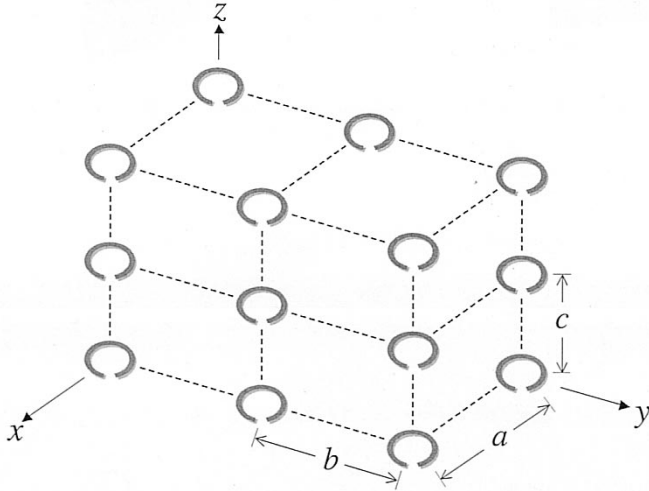


Fig. 1. 3-D array of inclusions whose dielectric constant is ϵ_r , and conductivity is σ . Host material has a dielectric constant ϵ_b .

a wavelength. For our calculations, the spacings near the resonance frequency in Fig. 6 are 0.1λ , which is generally accepted as the limit for quasi-static Lorentz theory [23]. Beyond the resonance frequency, the Lorentz theory becomes increasingly less accurate. It should be noted that for the Lorentz theory, the inclusion size should also be much smaller than the spacing.

The 6×6 constitutive relation matrix is expressed in terms of the interaction matrix and the polarizability matrix which can be numerically calculated by using the existing electromagnetic codes. Examples of split ring resonators and an array of helices are shown to illustrate a negative refractive index medium and a chiral medium. Numerical examples are also used to verify the consistency constraint and the reciprocity relations for a bianisotropic medium. This paper shows a method of calculating those constitutive relations for a given metamaterial and composite medium. This is obviously a first step toward designing and producing metamaterials with desired characteristics. In this paper, we use the time dependence of $\exp(j\omega t)$.

II. FORMULATION OF THE PROBLEM

Let us consider a medium consisting of a 3-D periodic array of inclusions in a host material (Fig. 1). Each inclusion may be a wire, a ring, a helix, or a split ring proposed by Pendry *et al.* [1]. The spacings along x , y , and z directions are a , b , and c , respectively. Under the influence of an applied electromagnetic field, the inclusion produces electric and magnetic multipoles. In this paper, to be consistent with the Lorentz theory [23], we limit ourselves to the electric and magnetic dipoles expressed in a quasi-static approximation.

Let us first note that in the E - B representation, we have in general

$$\begin{aligned} \bar{D} &= \epsilon_0 \bar{E} + \bar{P}(\bar{E}, \bar{B}) \\ \bar{H} &= \frac{1}{\mu_0} \bar{B} - \bar{M}(\bar{E}, \bar{B}) \end{aligned} \quad (6)$$

where the electric polarization \bar{P} and the magnetic polarization \bar{M} are functions of \bar{E} and \bar{B} . In the Lorentz theory, we only consider the dipole term representing each inclusion immersed

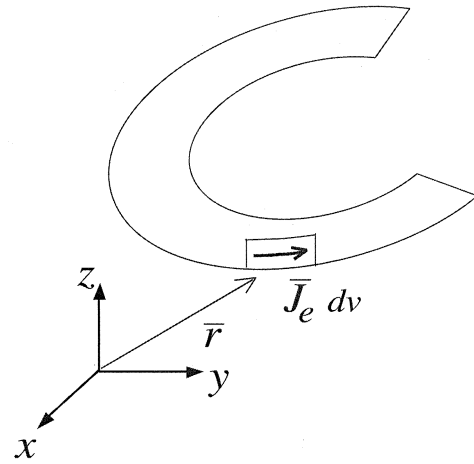


Fig. 2. Current \bar{J}_e on the inclusion produced by the effective field \bar{E}_ℓ . Current \bar{J}_m is also produced by the effective field \bar{B}_ℓ .

in the uniform effective field $(\bar{E}_\ell, \bar{B}_\ell)$. The effective field $(\bar{E}_\ell, \bar{B}_\ell)$ acts on the inclusion to produce the electric and magnetic dipoles. The effective field consists of the external applied field (\bar{E}, \bar{B}) and the interaction field (\bar{E}_i, \bar{B}_i) which are produced by all the inclusions except the particular inclusion under consideration in the infinite array.

\bar{P} and \bar{M} can then be expressed as:

$$\begin{aligned} \bar{P} &= N \bar{p} \\ \bar{M} &= N \bar{m} \end{aligned} \quad (7)$$

where $N = (abc)^{-1}$ is the number of inclusions per unit volume, and \bar{p} and \bar{m} are the electric and magnetic dipole moments of each inclusion produced by the effective field $(\bar{E}_\ell, \bar{B}_\ell)$. The dipole moments are then given by the generalized polarizability matrix $[\bar{\alpha}]$ [11].

$$\begin{bmatrix} \bar{p} \\ \bar{m} \end{bmatrix} = [\bar{\alpha}] \begin{bmatrix} \bar{E}_\ell \\ \bar{B}_\ell \end{bmatrix} \quad (8)$$

where $[\bar{\alpha}] = \begin{bmatrix} \bar{\alpha}_{ee} & \bar{\alpha}_{em} \\ \bar{\alpha}_{me} & \bar{\alpha}_{mm} \end{bmatrix}$.

Note that \bar{p} , \bar{m} , \bar{E}_ℓ , and \bar{B}_ℓ are all 3×1 vectors and $[\bar{\alpha}]$ is a 6×6 matrix.

Let us examine the polarizability matrix $[\bar{\alpha}]$. The electric dipole moment \bar{p} and the magnetic dipole moment \bar{m} are produced by the effective field $(\bar{E}_\ell, \bar{B}_\ell)$. The field \bar{E}_ℓ produces the current \bar{J}_e and the field \bar{B}_ℓ produces the current \bar{J}_m on the inclusion (Fig. 2). In matrix form, we write

$$[\bar{p}] = \frac{1}{j\omega} \int dv ([\bar{J}_e][\bar{E}_\ell] + [\bar{J}_m][\bar{B}_\ell]) \quad (9)$$

$$[\bar{m}] = \frac{1}{2} \int dv \bar{r} \times ([\bar{J}_e][\bar{E}_\ell] + [\bar{J}_m][\bar{B}_\ell]). \quad (10)$$

Now we have the final expression for the polarizability matrix $[\bar{\alpha}]$

$$\begin{aligned} [\bar{\alpha}] &= \begin{bmatrix} \bar{\alpha}_{ee} & \bar{\alpha}_{em} \\ \bar{\alpha}_{me} & \bar{\alpha}_{mm} \end{bmatrix}, \\ \bar{\alpha}_{ee} &= \frac{1}{j\omega} \int dv [\bar{J}_e] \end{aligned}$$

$$\begin{aligned}\bar{\alpha}_{me} &= \frac{1}{2} \int dv \bar{r} \times [\bar{J}_e] \\ \bar{\alpha}_{em} &= \frac{1}{j\omega} \int dv [\bar{J}_m] \\ \bar{\alpha}_{mm} &= \frac{1}{2} \int dv \bar{r} \times [\bar{J}_m].\end{aligned}\quad (11)$$

Note that \bar{J}_e is the current density produced by the electric field $E_{\ell x} = E_{\ell y} = E_{\ell z} = 1(V/m)$ and thus the unit is $(A/m^2)/(V/m)$. Similarly, \bar{J}_m has the unit of $(A/m^2)/T(\text{tesla})$.

Let us next consider the effective field $(\bar{E}_\ell, \bar{B}_\ell)$. As discussed above, the effective field acts on the inclusion and produces the electric and the magnetic dipoles. The effective field consists of the external applied field (\bar{E}, \bar{B}) and the interaction field (\bar{E}_i, \bar{B}_i) .

$$\begin{bmatrix} \bar{E}_\ell \\ \bar{B}_\ell \end{bmatrix} = \begin{bmatrix} \bar{E} \\ \bar{B} \end{bmatrix} + \begin{bmatrix} \bar{E}_i \\ \bar{B}_i \end{bmatrix}.\quad (12)$$

The interaction field is produced by all the dipoles except the particular inclusion under consideration. For a 3-D array of inclusions consisting of the electric and magnetic dipoles, the interaction field (\bar{E}_i, \bar{B}_i) has been obtained and is given by [23]

$$\begin{bmatrix} \bar{E}_i \\ \bar{B}_i \end{bmatrix} = N[\bar{C}] \begin{bmatrix} \bar{p} \\ \bar{m} \end{bmatrix}.\quad (13)$$

The interaction constant matrix $[\bar{C}]$ is given by

$$[\bar{C}] = \begin{bmatrix} \frac{1}{\epsilon_0 \epsilon_b} \bar{C} & \bar{0} \\ \bar{0} & \mu_0 \bar{C} \end{bmatrix}\quad (14)$$

where $\bar{C} = 3 \times 3$ diagonal matrix = $\begin{bmatrix} C_x & 0 & 0 \\ 0 & C_y & 0 \\ 0 & 0 & C_z \end{bmatrix}$, and

$\bar{0} = 3 \times 3$ null matrix, and ϵ_b is the relative dielectric constant of the host material.

Substituting (8) and (13) into (12), we obtain

$$\begin{bmatrix} \bar{E}_\ell \\ \bar{B}_\ell \end{bmatrix} = \begin{bmatrix} \bar{E} \\ \bar{B} \end{bmatrix} + N[\bar{C}] [\bar{\alpha}] \begin{bmatrix} \bar{E}_\ell \\ \bar{B}_\ell \end{bmatrix}.\quad (15)$$

We then obtain

$$\begin{bmatrix} \bar{E}_\ell \\ \bar{B}_\ell \end{bmatrix} = [\bar{U} - N[\bar{C}] [\bar{\alpha}]]^{-1} \begin{bmatrix} \bar{E} \\ \bar{B} \end{bmatrix}\quad (16)$$

where $[\bar{U}]$ is a 6×6 unit matrix. Finally, \bar{D} and \bar{H} are given by

$$\begin{aligned}\bar{D} &= \epsilon_0 \epsilon_b \bar{E} + N\bar{p} \\ \bar{H} &= \frac{1}{\mu_0} \bar{B} - N\bar{m}.\end{aligned}\quad (17)$$

Substituting (8) and (16) into (17), we get

$$\begin{bmatrix} \bar{D} \\ \bar{H} \end{bmatrix} = \begin{bmatrix} \bar{\epsilon}_p & \bar{\alpha}_p \\ \bar{\beta}_p & \bar{\mu}_p^{-1} \end{bmatrix} \begin{bmatrix} \bar{E} \\ \bar{B} \end{bmatrix}$$

where

$$\begin{bmatrix} \bar{\epsilon}_p & \bar{\alpha}_p \\ \bar{\beta}_p & \bar{\mu}_p^{-1} \end{bmatrix} = \begin{bmatrix} \epsilon_0 \epsilon_b \bar{U} & \bar{0} \\ \bar{0} & \frac{1}{\mu_0} \bar{U} \end{bmatrix} + N \begin{bmatrix} \bar{U} & \bar{0} \\ \bar{0} & -\bar{U} \end{bmatrix} [\bar{\alpha}] [\bar{U} - N[\bar{C}] [\bar{\alpha}]]^{-1}\quad (18)$$

and $[\bar{U}]$ is a 3×3 unit matrix.

The constitutive relation (1) in E - H representation is then given by (3). This is the final expression for the generalized constitutive relations for a 3-D array of inclusions under quasi-static approximation. This is the generalization of the Lorentz-Lorenz formula and leads to the Maxwell-Garnett formula for randomly distributed spherical inclusions to be discussed in Section VI [21], [24].

III. INTERACTION MATRIX

The interaction matrix $[\bar{C}]$ for a 3-D array of dipoles with the spacing a , b , and c in the x , y , and z directions, respectively, (Fig. 1), has been obtained [23].

$$\begin{aligned}C_x &= f\left(\frac{b}{a}, \frac{c}{a}\right) = \left(\frac{b}{a}\right) \left(\frac{c}{a}\right) \left[\frac{\zeta(3)}{\pi} - S\left(\frac{b}{a}, \frac{c}{a}\right)\right] \\ C_y &= f\left(\frac{c}{b}, \frac{a}{b}\right) \\ C_z &= f\left(\frac{a}{c}, \frac{b}{c}\right)\end{aligned}\quad (19)$$

where

$$\zeta(z) = \sum_{k=1}^{\infty} k^{-z}, \quad \text{Re}\{z\} > 1 \text{ (Riemann Zeta function),}$$

$$S\left(\frac{b}{a}, \frac{c}{a}\right) = \frac{1}{\pi} \sum_{n=-\infty}^{\infty} \sum_{s=-\infty}^{\infty} \sum_{m=1}^{\infty} (2m\pi)^2 K_0 \left(2m\pi \left[\left(\frac{nb}{a}\right)^2 + \left(\frac{sc}{a}\right)^2 \right]^{1/2} \right).$$

K_0 is the modified Bessel function, and the term with $n = s = 0$ is excluded. For a cubic lattice, $a = b = c$ and we get $C_x = C_y = C_z = 1/3$. This is identical to the interaction constant used to derive the Clausius-Mosotti equation by calculating the internal field inside a spherical cavity surrounded by the dielectric with uniform polarization [21].

IV. QUASI-STATIC CALCULATION OF \bar{J}_e AND \bar{J}_m

As can be seen from (9) and (10), the current \bar{J}_e on the inclusion is produced by \bar{E}_ℓ and the current \bar{J}_m is produced by \bar{B}_ℓ , and these two currents are independently produced under quasi-static approximation.

In order to calculate \bar{J}_m , we apply a uniform magnetic field on the inclusion and calculate the current. For example, for the magnetic field $\bar{B}_\ell = B_0 \hat{z}$, we need to have the incident field B_0 which is uniform throughout the space $a \times b \times c$ and the electric field is zero. Since we have electromagnetic codes which can calculate the current on the inclusion with a plane wave incidence, it is convenient to make use of these existing codes. However, a plane wave does not give a uniform magnetic field. To obtain a uniform magnetic field, we use the incident plane waves from several symmetric directions as shown in Fig. 3. The electric field at or near the inclusion is cancelled out and nearly zero, and the magnetic field is close to uniform. The current \bar{J}_m is then numerically calculated. We found that the incident fields from four directions give a nearly uniform magnetic field for a

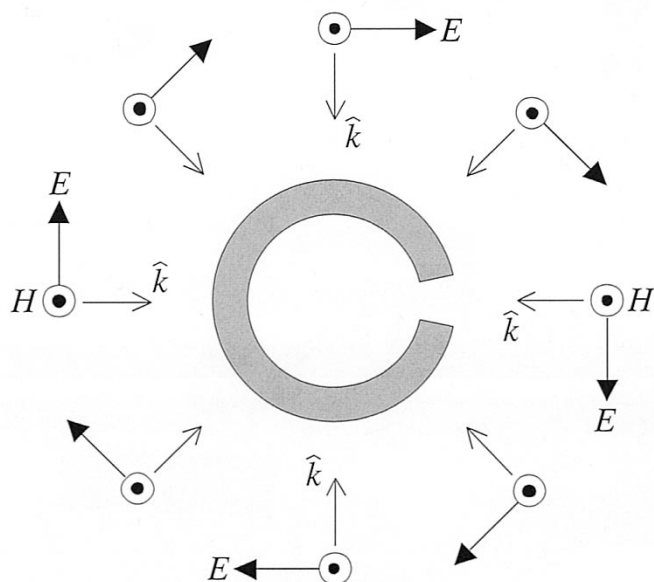


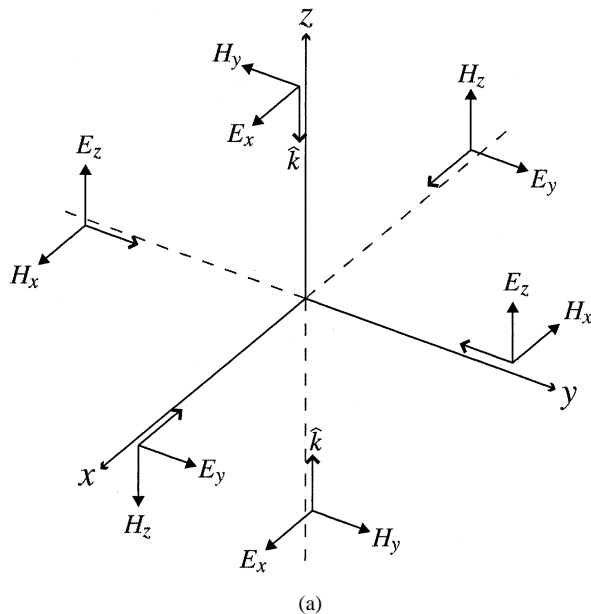
Fig. 3. Incident plane waves from several symmetric directions produce an almost uniform magnetic field on the inclusion.

ring type structure shown in Fig. 3, and the fields from eight directions appear to offer little advantage over the four incident fields. However, the number of the incident plane waves for a different structure must be carefully chosen.

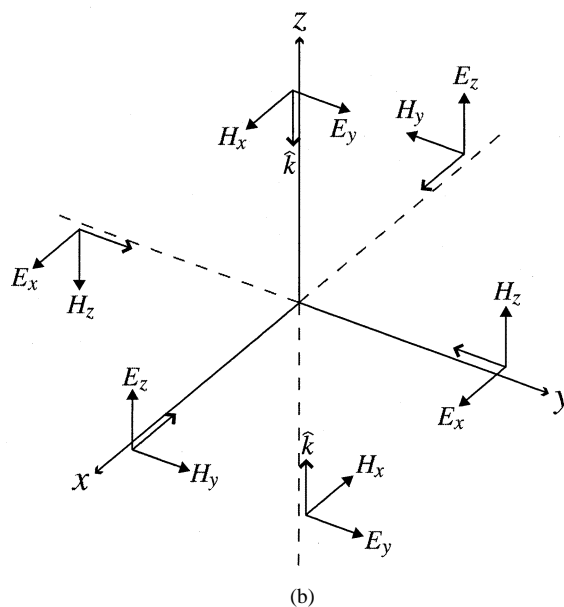
In general, in order to calculate all 6×6 elements of the polarizability matrix $[\bar{\alpha}]$ in (11), we need to have $E_x, E_y, E_z, H_x, H_y,$ and H_z which are uniform throughout the space $a \times b \times c$. One scheme is to have three incident plane waves along the $x, y,$ and z axes as shown in Fig. 4. By taking the sum and the difference, we can generate uniform $E_x, E_y, E_z, H_x, H_y,$ and H_z . Note that by using the scheme in Fig. 4(a) and (b), four plane waves are combined to give a nearly uniform field for each of six components. For example, to get uniform E_x , we take the sum of two plane waves along the z axis propagating in opposite directions in Fig. 4(a) and take the sum of two plane waves along the y axis propagating in opposite directions in Fig. 4(b). Note that for plane wave, \vec{B} and \vec{H} are simply related by $\vec{B} = \mu_0 \vec{H}$. The schemes shown in Figs. 3 and 4 are convenient because we can make use of existing electromagnetic codes of plane wave incidence. However, its limitations are that the effective field used to calculate the polarizability matrix is nearly uniform only over small inclusions of size less than 0.1λ . To improve the accuracy of our quasi-static calculations, a more complete quasi-static analysis such as given in [25] is necessary. It should also be pointed out that the magnetic polarizability (10) is given by the volume integral of the form

$$\int dv \vec{r} \times \vec{J}. \quad (20)$$

Even though this is independent of the choice of origin for the magnetostatic case where $\nabla \cdot \vec{J} = 0$, in general, this integral depends on the choice of origin. Therefore, the origin should be chosen at the center of gravity of the geometric shape of the inclusion.



(a)



(b)

Fig. 4. (a) A pair of two plane waves along $+z$ and $-z$ directions produces uniform E_x when summed, and uniform H_y when differences are taken. Similarly, $E_y \times H_z$ along $+x$ and $-x$ directions give uniform E_y and H_z , and $E_z \times H_x$ along $+y$ and $-y$ directions give uniform E_z and H_x . (b) Similarly, the waves shown here give additional plane waves which, together with (a), produce nearly uniform effective fields.

V. CURRENT \vec{J}_e AND \vec{J}_m

If the inclusion has a complex relative dielectric constant ϵ , and the host material has a relative dielectric constant ϵ_b , then the current is given by

$$\vec{J} = j\omega\epsilon_0(\epsilon - \epsilon_b)\vec{E}. \quad (21)$$

We can express the dielectric constant by

$$\begin{aligned} \epsilon &= \epsilon_r - j\epsilon_i \\ &= \epsilon_r - j \frac{\sigma}{\omega\epsilon_0}. \end{aligned} \quad (22)$$

And then, we have

$$\bar{\mathbf{J}} = j\omega\epsilon_0(\epsilon_r - \epsilon_b)\bar{\mathbf{E}} + \sigma\bar{\mathbf{E}}. \quad (23)$$

In the quasi-static approximation, the displacement current is often negligible, and we have approximately

$$\bar{\mathbf{J}} = \sigma\bar{\mathbf{E}}. \quad (24)$$

It is also clear that if the inclusion is a wire, we use

$$\int dv \bar{\mathbf{J}} = \int dl I \quad (25)$$

where I is the current on the wire.

VI. SPHERICAL INCLUSIONS AND MAXWELL-GARNETT FORMULA

Even though our interest is in obtaining the constitutive relations for inclusions of complex shape, it may be instructive to verify that the general formula (18) reduces to the conventional Maxwell-Garnett formula for a spherical case. If the inclusions are axially symmetric such as a prolate spheroid with major axis in the z direction, then the coupling terms $\bar{\alpha}_{em}$ and $\bar{\alpha}_{me}$ disappear and $\bar{\alpha}_{ee}$ and $\bar{\alpha}_{mm}$ become diagonal. Therefore, the constitutive relations are reduced to $\bar{\mathbf{D}} = \bar{\epsilon}\bar{\mathbf{E}}$ and $\bar{\mathbf{B}} = \bar{\mu}\bar{\mathbf{H}}$. For an ellipsoidal inclusion, $\bar{\alpha}_{ee}$ is well known [21] and we get

$$\bar{\epsilon} = \epsilon_0\epsilon_b\bar{\mathbf{U}} + N\bar{\epsilon}_{ee} \left[\bar{\mathbf{U}} - \frac{N\bar{\mathbf{C}}}{\epsilon_0\epsilon_b}\bar{\epsilon}_{ee} \right]^{-1}. \quad (26)$$

In particular, for a spherical inclusion with radius a_0 in a cubic lattice, the interaction constant is $1/3$, and we get

$$\bar{\alpha}_{ee} \rightarrow \frac{3(\frac{\epsilon}{\epsilon_b} - 1)}{\frac{\epsilon}{\epsilon_b} + 2}\epsilon_0\epsilon_b V, \quad V = \frac{4\pi a_0^3}{3}. \quad (27)$$

With (27), (26) becomes scalar and reduces to the Maxwell-Garnett formula.

Similarly, we can get the Maxwell-Garnett formula for the permeability. For a spherical inclusion, the lowest order electric field inside the sphere in the uniform effective field $H_0\hat{z}$ is given by [25]

$$\bar{\mathbf{E}} = (-j\omega\mu_0 H_0)\frac{\rho}{2}\hat{\phi} \quad (28)$$

using the cylindrical system (ρ, ϕ, z) .

The current $\bar{\mathbf{J}}_m$ is, therefore

$$\bar{\mathbf{J}}_m = j\omega\epsilon_0(\epsilon - \epsilon_b)(-j\omega\mu_0 H_0)\frac{\rho}{2}\hat{\phi}. \quad (29)$$

Substituting this in (11) and performing integration, we get

$$\alpha_{mm} = \mu_0(k_0 a_0)^2(\epsilon - \epsilon_b)\frac{V}{10}. \quad (30)$$

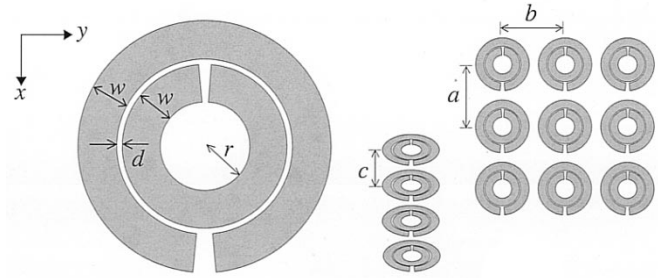


Fig. 5. Split ring resonator (SRR) and definitions of distances [1].

We then get

$$\mu = \mu_0 + N\alpha_{mm} \left[1 - \frac{N}{3\mu_0}\alpha_{mm} \right]^{-1} \quad (31)$$

which is the Maxwell-Garnett formula for permeability for the medium with spherical inclusions. Note that α_{mm} is proportional to $(k_0 a_0)^2$ and becomes small for low frequencies. A more complete analysis for magnetoquasi-static solutions for a prolate spheroid has been given recently [25].

VII. SPLIT RING RESONATOR

As an example, we consider a 3-D array of split ring resonators (SRRs) (Fig. 5). Using the scheme shown in Fig. 3, the uniform effective magnetic field is excited and μ' and μ'' are calculated at different frequencies with the formulation described in Section II, which are shown in Fig. 6(a). Similarly, taking the difference between two opposing plane waves, we calculate ϵ' and ϵ'' , which are shown in Fig. 6(b).

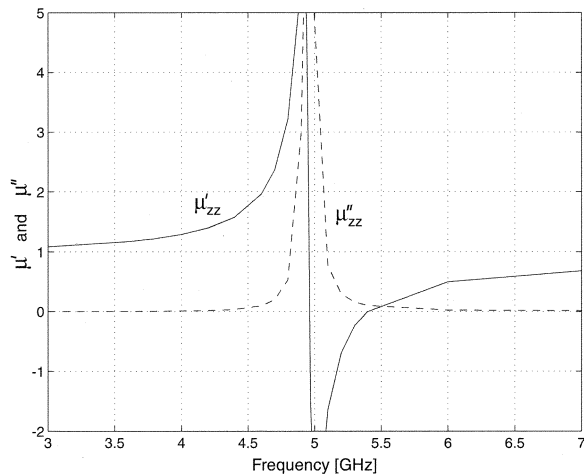
In this example, $\bar{\mathbf{B}}_\ell = B_{\ell z}\hat{z}$ and $\bar{\mathbf{E}}_\ell = E_{\ell x}\hat{x} + E_{\ell y}\hat{y}$. Therefore, writing $\bar{\epsilon} = [\epsilon_{ij}]$, $\bar{\xi} = [\xi_{ij}]$, $\bar{\zeta} = [\zeta_{ij}]$, and $\bar{\mu} = [\mu_{ij}]$ with i and $j = x, y, z$, we calculated

$$\begin{aligned} \epsilon_{xx} &= \epsilon'_{xx} - j\epsilon''_{xx} \\ \epsilon_{yy} &= \epsilon'_{yy} - j\epsilon''_{yy} \\ \mu_{zz} &= \mu'_{zz} - j\mu''_{zz}. \end{aligned} \quad (32)$$

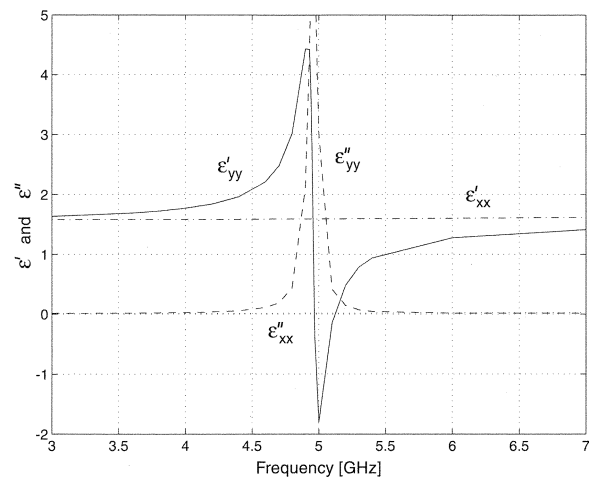
It is interesting to note the resonance behaviors discussed by Pendry, Smith and others. Also noted are the negative permeability and permittivity near resonance frequency, which have strong dispersive characteristics as already discussed by several workers [1]–[3], [5]. The SRR used here has the same dimensions as that in [2], and its resonance frequency in Fig. 6 is close to that of [2] with selected spacings. Note that the resonance frequency is dependent on the spacings as well as the size [1], and according to our calculation, if c is increased by 10%, then the resonance frequency is increased by about 3%. In Fig. 6(b), it can be found that ϵ_{yy} shows an analogous resonance curve to that of μ_{zz} whereas ϵ_{xx} is almost constant, which agrees with the theoretical analysis by Marqués *et al.* [6].

If a plane wave with E_y and H_z is propagating in the x direction in this medium, the refractive index is given by

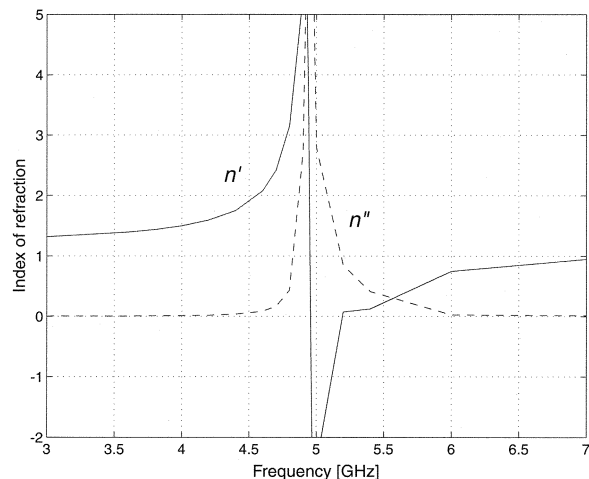
$$n = (\epsilon_{yy}\mu_{zz})^{1/2} = n' - jn''. \quad (33)$$



(a)



(b)



(c)

Fig. 6. Plot of μ , ϵ , and n of a SRR medium. $r = 1.5$ mm, $w = 0.8$ mm, $d = 0.2$ mm, $a = b = 8$ mm, and $c = 3.9$ mm. The conductivity of the ring is 5.8×10^7 [S/m]. The thickness of the ring is much greater than the skin depth.

This is shown in Fig. 6(c). Note that n' becomes negative in the frequency range above the resonance, and the phase velocity

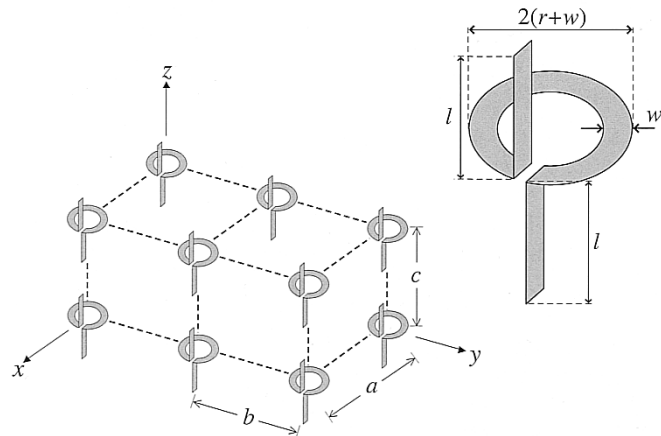


Fig. 7. 3-D array of helices. $r = 1.5$ mm, $w = 0.8$ mm, $l = 3$ mm. $a = b = c = 8$ mm.

$v_p = c_0/n$ is negative, where c_0 is the velocity of light. However, the group velocity given by

$$\frac{v_g}{c_0} = \left[\frac{\partial(\omega n')}{\partial \omega} \right]^{-1} \quad (34)$$

is positive representing the signal velocity, except in the region very close to the resonance, where the group velocity becomes negative. This is the anomalous dispersion region, and the group velocity does not represent the signal velocity. The phase velocity, the group velocity (34) and the signal velocity in the anomalous dispersion region have been extensively discussed by Brillouin [26].

VIII. CHIRAL MEDIUM CONSISTING OF AN ARRAY OF HELICES

We consider a 3-D array of helices [11], [12], [14]–[16] (Fig. 7). We calculated all 6×6 matrix elements. Note that the dimensions of $\bar{\xi}$ and $\bar{\zeta}$ are both $\gamma \mu_0 = \sqrt{\mu_0 \epsilon_0} = c_0^{-1}$, and therefore we normalized all elements of $\bar{\xi}$ and $\bar{\zeta}$ by c_0^{-1} . $\bar{\epsilon}$ and $\bar{\mu}$ are normalized with ϵ_0 and μ_0 , respectively.

Our calculations show at 8 GHz

$$\begin{aligned} \frac{\bar{\epsilon}}{\epsilon_0} &= \begin{bmatrix} 1.20 - j0.01 & 0 & 0 \\ 0 & 0.77 - j0.08 & 0.47 + j0.10 \\ 0 & 0.47 + j0.10 & 0.48 - j0.15 \end{bmatrix} \\ \frac{\bar{\xi}}{\gamma \mu_0} &= \begin{bmatrix} 0 & 0 & 0 \\ 0 & -0.01 + j0.05 & 0.10 - j0.37 \\ 0 & 0.02 - j0.05 & -0.13 + j0.54 \end{bmatrix} \\ \frac{\bar{\zeta}}{\gamma \mu_0} &= \begin{bmatrix} 0 & 0 & 0 \\ 0 & 0.01 - j0.05 & -0.02 + j0.06 \\ 0 & -0.10 + j0.40 & 0.14 - j0.56 \end{bmatrix} \\ \frac{\bar{\mu}}{\mu_0} &= \begin{bmatrix} 1.00 - j0.00 & 0 & 0 \\ 0 & 0.99 - j0.00 & 0.06 + j0.01 \\ 0 & 0.06 + j0.01 & 0.50 - j0.13 \end{bmatrix}. \end{aligned} \quad (35)$$

From that, we get

$$\begin{aligned}\text{Trace}(\overline{[\xi]}[\overline{[\mu]}]^{-1}) &= (-0.57 + j1.04) \times \gamma \\ \text{Trace}(\overline{[\mu]}^{-1}[\overline{[\zeta]}) &= (0.60 - j1.08) \times \gamma\end{aligned}\quad (36)$$

which satisfy (4) with less than 5% difference. The elements designated by 0 are negligibly small. Since the polarizability matrices $\overline{\alpha}_{ee}$, $\overline{\alpha}_{em}$, $\overline{\alpha}_{me}$, and $\overline{\alpha}_{mm}$ are independently calculated from six components of $(\overline{E}_\ell, \overline{B}_\ell)$, (36) provides an independent check on the accuracy of the numerical calculation.

The elements (35) are for right-handed helices shown in Fig. 7. We also calculated all 36 elements for left-handed helices as follows:

$$\begin{aligned}\overline{[\epsilon]} &= \begin{bmatrix} 1.20 - j0.01 & 0 & 0 \\ 0 & 0.78 - j0.08 & -0.46 - j0.10 \\ 0 & -0.48 - j0.10 & 0.48 - j0.15 \end{bmatrix} \\ \overline{[\xi]} &= \begin{bmatrix} 0 & 0 & 0 \\ 0 & 0.01 - j0.05 & 0.10 - j0.38 \\ 0 & 0.01 - j0.05 & 0.14 - j0.54 \end{bmatrix} \\ \overline{[\zeta]} &= \begin{bmatrix} 0 & 0 & 0 \\ 0 & -0.01 + j0.05 & -0.02 + j0.06 \\ 0 & -0.10 + j0.40 & -0.14 + j0.56 \end{bmatrix} \\ \overline{[\mu]} &= \begin{bmatrix} 1.00 - j0.00 & 0 & 0 \\ 0 & 0.99 - j0.00 & -0.06 - j0.01 \\ 0 & -0.06 - j0.01 & 0.50 - j0.13 \end{bmatrix}\end{aligned}\quad (37)$$

and

$$\begin{aligned}\text{Trace}(\overline{[\xi]}[\overline{[\mu]}]^{-1}) &= (0.57 - j1.03) \times \gamma \\ \text{Trace}(\overline{[\mu]}^{-1}[\overline{[\zeta]}) &= (-0.60 + j1.08) \times \gamma.\end{aligned}\quad (38)$$

We note that the reciprocity relations (5) are satisfied for (35) and (37). Also we note that for the right-handed and the left-handed medium, the diagonal elements of $\overline{\epsilon}$ and $\overline{\mu}$ are the same, while the off-diagonal elements have opposite sign, and the diagonal elements of $\overline{\xi}$ and $\overline{\zeta}$ have opposite sign, while the off-diagonal elements are the same. These observations are useful to check the accuracy of the calculations.

IX. CONCLUSION

In this paper, we derived the generalized constitutive relations (18) for metamaterials consisting of a 3-D array of inclusions of arbitrary shape. This formula is derived under quasi-static approximation based on the Lorentz theory and is applicable to the spacing between the inclusions, which are small compared with a wavelength. Calculations of all elements of the matrix (18) can be made using the interaction matrix (19) for given spacings and the polarizability matrix (11) which is calculated using three incident plane waves along the x , y , and z axes as shown in the scheme in Fig. 4. Some numerical examples using an array of split ring resonators and a chiral array of helices are shown to illustrate the usefulness of the formulation and to verify the consistency constraint (4) and reciprocity relations (5). It should be noted that if the inclusion size and spacing increase, the multipole moments and the propagating constant

need to be included, requiring a complete full wave analysis [23].

REFERENCES

- [1] J. B. Pendry, A. J. Holden, D. J. Robbins, and W. J. Stewart, "Magnetism from conductors and enhanced nonlinear phenomena," *IEEE Trans. Microwave Theory Tech.*, vol. 47, pp. 2075–2084, 1999.
- [2] D. R. Smith, W. J. Padilla, D. C. Vier, S. C. Nemat-Nasser, and S. Schultz, "Composite medium with simultaneously negative permeability and permittivity," *Phys. Rev. Lett.*, vol. 84, no. 18, pp. 4184–4187, 2000.
- [3] V. G. Vesalago, "The electrodynamics of substances with simultaneously negative values of ϵ and μ ," *Sov. Phys. Usp.*, vol. 10, no. 4, pp. 509–514, 1968.
- [4] J. B. Pendry, "Negative refraction makes a perfect lens," *Phys. Rev. Lett.*, vol. 85, pp. 3966–3969, 2000.
- [5] R. A. Shelby, D. R. Smith, and S. Schultz, "Experimental verification of a negative index of refraction," *Science*, vol. 292, pp. 77–79, 2001.
- [6] R. Marqués, F. Medina, and R. Rafii-El-Idrissi, "Role of bianisotropy in negative permeability and left-handed metamaterials," *Phys. Rev. B*, vol. 65, pp. 144 440-1–144 440-6, 2002.
- [7] R. W. Ziolkowski and E. Heyman, "Wave propagation in media having negative permittivity and permeability," *Phys. Rev. E*, vol. 64, p. 056 625, 2001.
- [8] F. Wu and K. W. Whites, "Quasistatic effective permittivity of periodic composites containing complex shaped dielectric particles," *IEEE Trans. Antennas Propagat.*, vol. 49, pp. 1174–1182, 2001.
- [9] B. Sareni, L. Krahenbuhl, A. Beroual, and A. Nicolas, "A boundary integral equation method for the calculation of the effective permittivity of periodic composites," *IEEE Trans. Magn.*, vol. 33, pp. 1580–1583, 1997.
- [10] A. Lakhtakia, V. K. Varadan, and V. V. Varadan, *Time-Harmonic Electromagnetic Fields in Chiral Media*, NY: Springer Verlag, 1989.
- [11] I. V. Lindell, A. H. Sihvola, S. A. Tretyakov, and A. J. Viitanen, *Electromagnetic Waves in Chiral and Bi-Isotropic Media*, MA: Artech, 1994.
- [12] V. V. Varadan, A. Lakhtakia, and V. K. Varadan, "Equivalent dipole moments of helical arrangements of small, isotropic, point-polarizable scatterers: Application to chiral polymer design," *J. Appl. Phys.*, vol. 63, pp. 280–284, 1988.
- [13] N. Engheta, D. L. Jaggard, and M. W. Kowarz, "Electromagnetic waves in Faraday chiral media," *IEEE Trans. Antennas Propagat.*, vol. 40, pp. 367–374, 1992.
- [14] A. J. Bahr and K. R. Clausing, "An approximate model for artificial chiral material," *IEEE Trans. Antennas Propagat.*, vol. 42, pp. 1592–1599, 1994.
- [15] F. Mariotte, S. A. Tretyakov, and B. Sauviac, "Isotropic chiral composite modeling: Comparison between analytical, numerical, and experimental results," *Microwave Opt. Tech. Lett.*, vol. 7, pp. 861–864, 1994.
- [16] S. A. Tretyakov, F. Mariotte, C. R. Simovski, T. G. Kharina, and J.-P. Heliot, "Analytical antenna model for chiral scatterers: Comparison with numerical and experimental data," *IEEE Trans. Antennas Propagat.*, vol. 44, pp. 1006–1014, 1996.
- [17] A. Lakhtakia, "On perfect lenses and nihility," *Int. J. Infrared Millim. Waves*, vol. 23, pp. 339–343, 2002.
- [18] W. S. Weiglhofer, "Constitutive relations," in *Proc. SPIE*, vol. 4806, 2002, pp. 67–80.
- [19] J. Kong, *Electromagnetic Wave Theory*. New York: Wiley, 1986.
- [20] J. A. Kong, "Theorems of bianisotropic media," *Proc. IEEE*, vol. 60, no. 9, pp. 1036–1046, 1972.
- [21] A. Ishimaru, *Electromagnetic Wave Propagation, Radiation, and Scattering*. Englewood Cliffs, NJ: Prentice-Hall, 1991.
- [22] W. S. Weiglhofer and A. Lakhtakia, "A brief review of a new development for constitutive relations of linear bi-anisotropic media," *IEEE Antennas Propagat. Mag.*, vol. 37, pp. 32–35, 1995.
- [23] R. E. Collin, *Field Theory of Guided Waves*. New York: IEEE, 1991, ch. 12.
- [24] B. Michel, A. Lakhtakia, W. S. Weiglhofer, and T. G. Mackay, "Incremental and differential maxwell garnett formalisms for bi-anisotropic composites," *Composites Sci. Tech.*, vol. 61, pp. 13–18, 2001.
- [25] H. Braunisch, C. O. Ao, K. O'Neill, and J. A. Kong, "Magnetoquasistatic response of conducting and permeable prolate spheroid under axial excitation," *IEEE Trans. Geosci. Remote Sensing*, vol. 39, pp. 2689–2701, 2001.
- [26] L. Brillouin, *Wave Propagation and Group Velocity*. New York: Academic, 1960.



Akira Ishimaru (M'58–SM'63–F'73–LF'94) received the B.S. degree in 1951 from the University of Tokyo, Tokyo, Japan, and the Ph.D. degree in electrical engineering in 1958 from the University of Washington, Seattle.

From 1951 to 1952, he was with the Electrotechnical Laboratory, Tanashi, Tokyo, and in 1956, he was with Bell Laboratories, Holmdel, NJ. In 1958, he joined the faculty of the Department of Electrical Engineering, University of Washington, where he was Professor of electrical engineering and Adjunct

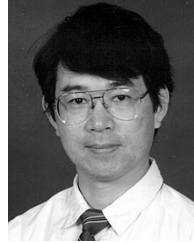
Professor of applied mathematics, and currently is Professor Emeritus. He has also been a Visiting Associate Professor with the University of California, Berkeley. His current research includes waves in random media, remote sensing, object detection and imaging in clutter environment, inverse problems, millimeter wave and optical propagation and scattering in the atmosphere and the terrain, rough surface scattering, and optical diffusion in tissues. He is the author of *Wave Propagation and Scattering in Random Media* (New York: Academic, 1978; IEEE Press-Oxford University Press Classic reissue, 1997) and *Electromagnetic Wave Propagation, Radiation, and Scattering* (Englewood Cliffs, NJ: Prentice-Hall, 1991).

Dr. Ishimaru has served as a member-at-large of the U.S. National Committee (USNC) and was chairman (1985–87) of Commission B of the USNC/International Union of Radio Science. He was editor (1979–1983) of *Radio Science* and Founding Editor of *Waves in Random Media*, Institute of Physics, United Kingdom. He is a Fellow of the Optical Society of America, the Acoustical Society of America, and the Institute of Physics, United Kingdom. He was the recipient of the 1968 IEEE Region VI Achievement Award and the IEEE Centennial Medal in 1984. He was appointed as Boeing Martin Professor in the College of Engineering in 1993. In 1995, he was awarded the Distinguished Achievement Award from the IEEE Antennas and Propagation Society. He was elected to the National Academy of Engineering in 1996. In 1998, he was awarded the Distinguished Achievement Award from the IEEE Geoscience and Remote Sensing Society. He is the recipient of the 1999 IEEE Heinrich Hertz Medal and the 1999 URSI Dellinger Gold Medal. In 2000, he received the IEEE Third Millennium Medal.



Seung-Woo Lee received the B.S. and M.S. degrees in electrical engineering from Seoul National University, Korea, in 1994 and 1996, respectively, and the Ph.D. degree in electrical engineering from the University of Washington, Seattle, in 2002.

He is currently working as a Research Associate with the University of Washington. His research interests include rough surface and random media scattering, target detection and imaging, artificial materials, and high-frequency devices.



Yasuo Kuga (S'79–M'83–SM'90) received the B.S., M.S., and Ph.D. degrees from the University of Washington, Seattle, in 1977, 1979, and 1983, respectively.

From 1983 to 1988, he was a Research Assistant Professor of electrical engineering at the University of Washington, where, since 1991, he has been a Professor of electrical engineering. From 1988 to 1991, he was an Assistant Professor of electrical engineering and computer science at The University of Michigan. His research interests are in the areas of microwave and millimeter-wave remote sensing, high-frequency devices and materials, and optics.

Dr. Kuga was an Associate Editor of *Radio Science* (1993–1996) and the *IEEE TRANSACTIONS ON GEOSCIENCE AND REMOTE SENSING* (1996–2000).



Vikram Jandhyala (M'00) received the B.Tech. degree in electrical engineering from IIT Delhi, India, in 1993 and the M.S. and Ph.D. degrees from the University of Illinois at Urbana-Champaign, in 1995 and 1998, respectively. As part of his graduate work, he co-developed the steepest-descent fast-multipole method.

Currently, he is an Assistant Professor with the Department of Electrical Engineering, University of Washington. His research interests include several aspects of computational and applied electromagnetics, including integral equation techniques, fast computational algorithms, high-speed circuits and devices, coupled simulation, signal integrity, and scattering computation. From 1998 to 2000 he was a Research and Development Engineer with Ansoft Corporation, Pittsburgh, PA. He was involved in the acceleration of Ansoft's integral equation solvers, and codeveloped a fast-multipole-based integral equation solver for Ansoft's Spicelink version 4.0 which was released in June 1999. He has published a book chapter and more than 60 journal papers and papers in refereed conference proceedings, and serves as a reviewer for several IEEE Transactions and conferences.

Dr. Jandhyala is a full Member of URSI Commission B. He is a recipient of the NSF CAREER Grant (2001), an Outstanding Graduate Research Award at UIUC (1998), and an IEEE Microwave Graduate Fellowship (1996–1997).